

# Quality Assessment of Terrestrial Laser Scanner Surface Deviation Analysis in Vegetation Slope Monitoring

Mohd Azwan Abbas, Albert K. Chong, Mohamad Aizat Asyraff Mohamad Azmi, Nursyahira Ahmad Fuad, Anuar Aspuri, Mohd Faizi Mohd Salleh, Zulkepli Majid, Khairulnizam M. Idris, Yusuf Drisu Opaluwa, Mohamad Asrul Mustafar, Norshahrizan Mohd Hashim, and Saiful Aman Sulaiman

**Abstract**—Mechanised with ability to rapidly acquire three-dimensional (3D) data using non-contact measurement, terrestrial laser scanner (TLS) has become an option in landslide monitoring. Dense 3D point clouds provided from TLS has enable surface deviation analysis to rigidly examine the displacement that occurred on the monitored object. However, the existence of vegetation on land slope has become uncertainty in TLS measurement for landslide monitoring. To concretely measure the effect of vegetation, this study has performed two epoch landslide monitoring using tacheometry (for benchmarking) and TLS (Topcon GLS-2000) at Kulim Techno City, Kedah, Malaysia. Sixteen (16) artificial targets were well-distributed on the slope to determine the accuracy of the employed TLS, evaluate the capability of TLS to determine the stability of the slope and scrutinise the significant of vegetation uncertainties in TLS measurement. Results obtained revealed that Topcon GLS-2000 manage to obtained results that are statistically similar to tacheometry and provides 0.006m of accuracy. However, the presence of high incidence

angles in TLS measurement has limited the capability to identify the significant displacement of the targets. With the aid of F-variance ratio test, the study has statistically proved that vegetation uncertainty is able to decrease the quality of TLS data.

**Index Terms**—Quality assessment, landslide monitoring, surface deviation, terrestrial laser scanner

## I. INTRODUCTION

Deformation measurement provides the knowledge to understand, quantify and analyse any small movement in magnitude and direction of any object including earth based or manmade structures. Consciousness of this knowledge branch is crucial to avoid jeopardising the vulnerable objects regarding their stability and healthiness. As depicted in Fig. 1, failure in detecting deformation of the object leads to destruction of the structure and could cause casualty (e.g. collapsed manmade structure, broken concrete or earth dam, earthquake and landslide).

Landslide is becoming a common issue worldwide; and it can be defined as the deformation of a mass of rock, debris, or earth down a slope. Landslide occurs when the strength of the earth material that composes the slope has less forces than the gravity effect which eventually causes the down-slope movement of soil and rock [1]. Currently, there are two approaches available for land slope monitoring (Fig. 2), which are using geodetic or geotechnical [2] methods.



Fig. 1. Landslide event at Cameron Highland, Malaysia.

Manuscript received September 06, 2019.

M. A. Abbas is with Faculty of Architecture, Planning & Surveying, Universiti Teknologi MARA, 40450 Shah Alam, Malaysia. (Office: +604-9882265; e-mail: mohdazwanabbas@gmail.com).

A. K. Chong is with School of Civil Engineering & Surveying, University of Southern Queensland, Australia. (e-mail: chonga@usq.edu.au).

M. A. A. Mohamad Azmi is with Faculty of Architecture, Planning & Surveying, Universiti Teknologi MARA, 40450 Shah Alam, Malaysia. (e-mail: sraizatazmi@gmail.com).

N. Ahmad Fuad, is with Faculty of Built Environment & Surveying, Universiti Teknologi Malaysia, Malaysia. (e-mail: nursyahiraaf@gmail.com).

A. Aspuri, is with Faculty of Built Environment & Surveying, Universiti Teknologi Malaysia, Malaysia. (e-mail: anuaraspuri@gmail.com).

M. F. Mohd Salleh, is with Faculty of Built Environment & Surveying, Universiti Teknologi Malaysia, Malaysia. (e-mail: mohdfaizi@utm.my).

Z. Majid is with Faculty of Built Environment & Surveying, Universiti Teknologi Malaysia, Malaysia. (e-mail: zulkeplimajid@utm.my).

K. M. Idris is with Faculty of Built Environment & Surveying, Universiti Teknologi Malaysia, Malaysia. (e-mail: khairulnizami@utm.my).

Y. D. Opaluwa is with Department of Surveying & Geoinformatics, School of Environmental Technology, Federal University of Technology Minna, Nigeria. (e-mail: opaluwayd@futminna.edu.ng).

M. A. Mustafar is with Faculty of Architecture, Planning & Surveying, Universiti Teknologi MARA, 40450 Shah Alam, Malaysia. (e-mail: mohamadasrul@gmail.com).

N. Mohd Hashim is with Faculty of Architecture, Planning & Surveying, Universiti Teknologi MARA, 40450 Shah Alam, Malaysia. (e-mail: shahndcdb@gmail.com).

S. A. Sulaiman is with Faculty of Architecture, Planning & Surveying, Universiti Teknologi MARA, 40450 Shah Alam, Malaysia. (e-mail: saifulaman@salam.uitm.edu.my).

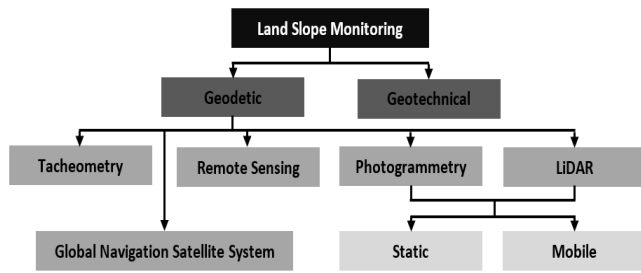


Fig. 2. Landslide monitoring approaches.

Tacheometry and global navigation satellite system (GNSS) methods can be considered as established geodetic approach in deformation measurement and landslide monitoring. Taking into account the accuracy in measurement, reliability of both methods have long been proven [3]-[6]. However, the precision (i.e. point density) provided from tacheometry and GNSS measurement is quite limited. To resolve that limitation, several non-contact measurement techniques were introduced, which are remote sensing [7], photogrammetry [8]-[9] and LiDAR [10]-[11]. With the capability to provide dense three-dimensional (3D) data (according to resolution of sensor), these measurement techniques have enabled surface to surface comparison assessment or often known as surface deviation analysis. This kind of analysis can homogeneously measure and identify the trend of movement that happened from two different measurement epochs. As illustrated in Fig. 3, instead of employing well distributed point to represent the whole surface, current approaches (which exploited dense data) can identify in detail, any changes that occurred at the object surface based on variation of colours' scale.

Other than employing mobile platform to carry the sensor, photogrammetry and LiDAR measurement methods are also utilised as static platform. Similar to tacheometry approach, ability to exploit static mode has reduced dependency on other instruments (i.e. inertial measurement units and GNSS) to acquire the position of mobile sensor. Less dependence can lessen propagation of errors which eventually yield good quality data. In other word, static measurement is able to offer better accuracy data than mobile based measurement.

Taking accuracy as first priority among those three approaches that are able to provide dense 3D data (i.e. remote sensing, photogrammetry and LiDAR), terrestrial laser scanner (static LiDAR) can be considered as the best. With significantly less error propagation in measurement and processing procedures, terrestrial laser scanner (TLS) is also not dependent upon the lighting conditions and surface texture as well as able to provide direct, rapid and high-density 3D data compared to other approaches [13]. However, according to Barbarella et al. [14], the presence of vegetation on the land slope can also cause errors in TLS measurement. Alba et al. [15] had reported the occurrence of such an error in TLS measurement due to the drastic change of monitored land surface caused by the growth of vegetation. Vegetation on slopes can be categorised under high and low types. For the high vegetation, it can be filtered based on the premise that they are significantly higher than their neighbourhoods [16]. Meanwhile, low vegetation is rather complicated for algorithms to differentiate between it

and the bare earth because the object is very close to the ground surface.

Based on the argument regarding low vegetation, it is important to investigate the significance of this kind of error sources in diminishing the accuracy of TLS measurement especially in landslide monitoring. There is a probability that this vegetation uncertainty can be neglected due to its less effect on TLS data. For that purpose, this study has robustly examined the accuracy of TLS data in landslide monitoring using the tacheometry measurement approach.

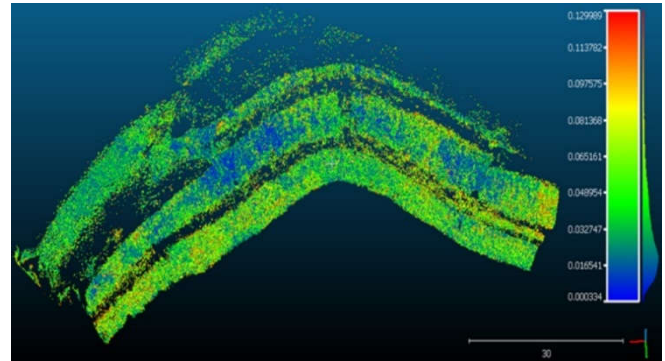


Fig. 3. Surface deviation analysis for landslide monitoring [12].

## II. TERRESTRIAL LASER SCANNER MEASUREMENT

Due to the interactive presentation and significant geometric information provided, 3D data acquisition has been widely employed in numerous applications which involved documentation, preservation, management, analysis and decision making. These include implementations that demand sub-centimetre geometric accuracy such as cultural heritage [17]-[19], surface reconstruction [20]-[21], structural deformation measurements [22]-[24], slope monitoring [14] and industrial measurements [25]-[26]. In contrast to traditional 3D data acquisition approaches (i.e. tacheometry and photogrammetry), terrestrial laser scanner is capable to rapidly acquire data without any requirement of direct contact with the object and extensive processing procedure. As visualised in Fig. 4 and similar to reflectorless tacheometry, TLS did measure three main components: i) Range ( $r$ ); ii) Horizontal direction ( $\phi$ ); and iii) Vertical angle ( $\theta$ ). According to Abbas et al. [27], there are three options employed by TLS in order to measure range: i) time-of-flight; ii) phase shift; and iii) triangulation. While the other components were obtained based on the scanner pre-determined axes.

To ensure that TLS data are significant for further processing, most of the TLSs on-board software have automatically convert raw TLSs data (i.e. spherical coordinate system) into Cartesian coordinate system. However, raw data in a spherical coordinate system is essential for this study to conduct least square adjustment for TLS data. With the aid of Fig. 5, conversion from Cartesian and spherical coordinates system can be expressed as follows [27]:

$$\begin{aligned} \text{Range, } r &= \sqrt{X_A^2 + Y_A^2 + Z_A^2} \\ \text{Horizontal\_direction, } \varphi &= \tan^{-1}\left(\frac{X_A}{Y_A}\right) \\ \text{Vertical\_angle, } \theta &= \tan^{-1}\left(\frac{Z_A}{\sqrt{X_A^2 + Y_A^2}}\right) \end{aligned} \quad (1)$$

While alternate conversions of both coordinates system are:

$$\begin{aligned} X_A &= r \times \cos(\varphi) \times \cos(\theta) \\ Y_A &= r \times \sin(\varphi) \times \cos(\theta) \\ Z_A &= r \times \sin(\theta) \end{aligned} \quad (2)$$

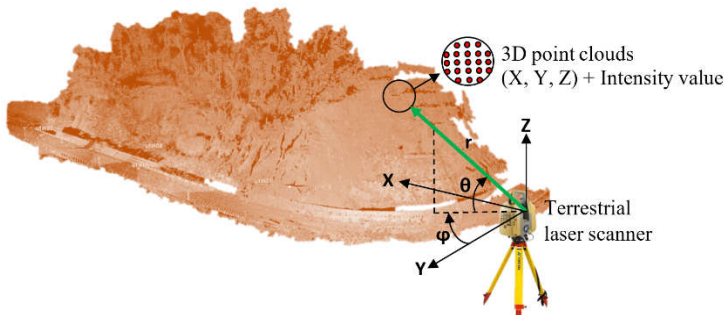


Fig. 4. Data collection using terrestrial laser scanner [18].

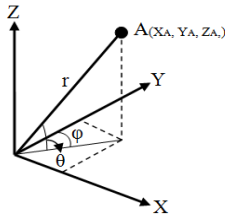


Fig. 5. Conversion between Cartesian and spherical coordinates system.

### III. EXPERIMENTS

Due to the active slope movement that occurred as reported by Kedah state authorities, this study was conducted at Kulim Techno City, Kedah, Malaysia. For benchmarking reason, as illustrated in Fig. 6, sixteen (16) artificial targets were well-distributed over the land slope area. Other than TLS measurement, this study also exploited conventional approach (i.e. reflectorless tacheometry) to establish 3D known coordinates for each target. Based on the reference coordinates obtained from tacheometry measurement, accuracy of TLS data can be mathematically determined.



Fig. 6. Research site located at Kulim Techno City, Kedah, Malaysia.

For the tacheometry measurement, Topcon ES-105 with accuracy of  $0.0014^\circ$  and 2mm for angular and range measurement, respectively was utilised to measure all the artificial targets. To secure the accuracy yielded, triangulation observation technique was employed (as shown in Fig. 7) and least squares adjustment has been entrusted to compute the most probable values of all targets along with their quality (i.e. precision).

As depicted in Fig. 7, Topcon GLS-2000 scanner was used to scan all targets with the surface of the land slope. According to the instrument specification sheet, this time-of-flight scanner utilised panoramic field-of-view to capture  $360^\circ$  of horizontal and  $270^\circ$  of vertical coverage. The accuracies of single point measurement are 3.5mm and  $0.0017^\circ$  for range and angular measurements, respectively. It should be noted that the accuracies mentioned above are based on single point measurement, if involves with the determination of target centroid procedure, the accuracy theoretically decreases due to the error propagation with other uncertainties during measurement phase [13], [28].

To measure the reliability of TLS in landslide monitoring, two (2) epochs of observations were carried out with an interval of a month. There are four analyses that were performed as follows:

- i. Transformation similarity analysis;
- ii. Dimensional discrepancies;
- iii. Displacement vector assessment; and
- iv. Surface deviation analysis.

#### A. Transformation similarity analysis

In this analysis, seven rigid transformation parameters are computed. The idea is to mathematically match the 3D points yielded from tacheometry (benchmark) and TLS data. Sixteen artificial targets from TLS are transformed into tacheometry coordinate system. To perform point to point analysis, Australis V6.06 software is used to implement rigid body transformation and subsequently calculate the RMS of the differences between control (tacheometry) and transformed coordinates (TLS). Smaller values of RMS for the calibrated data indicate that the quality of TLS data is closer to the reference values (results from tacheometry).

Utilising resection method, those artificial targets that have two coordinate systems derived from tacheometry and TLS can be employed to mathematically describe the relationship of those systems [9]:

$$X_i = T + S r x_i \quad (3)$$

where,

$X_i$  = 3D coordinates of targets in the TLS system.

$S$  = scale vector between two (2) systems.

$T$  = translation.

$r$  = rotation matrix.

$x_i$  = 3D coordinates of targets in the tacheometry system.

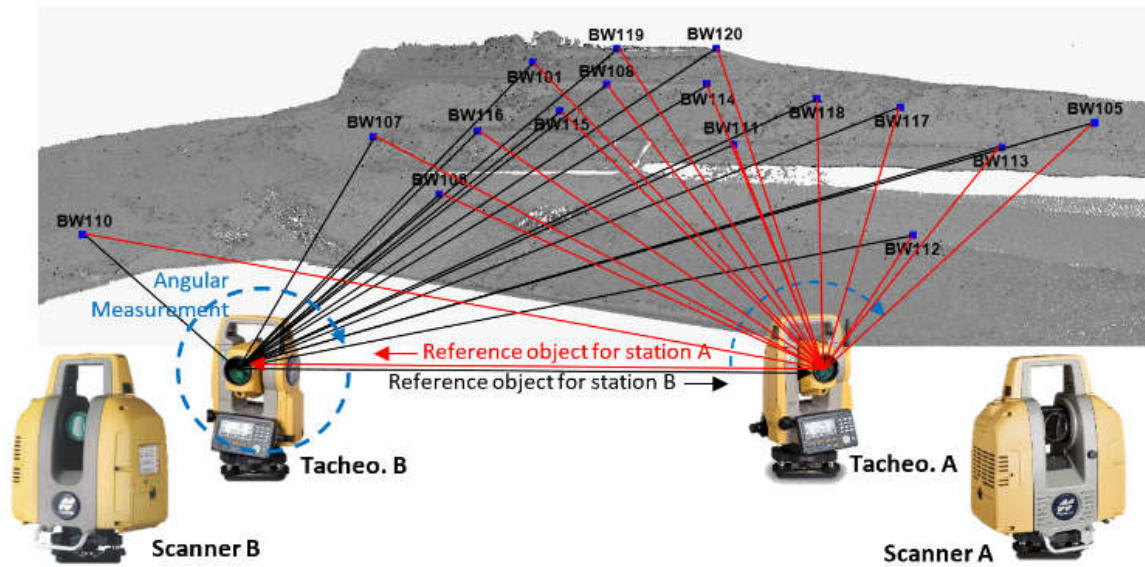


Fig. 7. Tacheometry and terrestrial laser scanner measurements for landslide monitoring.

*B. Dimensional Discrepancies*

This analysis sought assistance from accurate measurement technique (i.e. tacheometry) to measure the accuracy of TLS data. Fifteen independent dimensions were extracted from distributed sixteen artificial targets as depicted in Fig. 8. In order to measure the accuracy of TLS data, both sets of independent dimensions obtained from TLS and tacheometry are differentiated. Analysis of error was performed by computing standard deviation of the observation using the law of propagation of variance (LOPOV) [29].

*C. Displacement Vector Assessment*

With the determination to investigate the effect of vegetation in TLSs land slope monitoring, this study has carried out two epochs of measurement with an interval of one month. Information (3D coordinates of sixteen targets) obtained from two epochs measurement can be used to compute displacement vectors. Based on trigonometry formula, three-dimensional displacement can be derived as follow [27]:

$$\text{Displacement} = \sqrt{\Delta N^2 + \Delta E^2 + \Delta H^2} \quad (4)$$

where,

$$\Delta N = (N_{e2} - N_{e1})$$

$$\Delta E = (E_{e2} - E_{e1})$$

$$\Delta H = (H_{e2} - H_{e1})$$

$N_{e1}$ ,  $E_{e1}$  and  $H_{e1}$  = adjusted coordinates for first epoch.

$N_{e2}$ ,  $E_{e2}$  and  $H_{e2}$  = adjusted coordinates for second epoch.

Having two sets of displacement vectors (from TLS and tacheometry), integrity evaluation of TLS results were performed using statistical analysis. Selection of statistical test was made by taking into account the aim of this study which was to evaluate the similarity of the TLS displacement vectors and reference values (derived from tacheometry data). According to Ghilani [29], t distribution was used to compare population mean with the mean of a sample set based on the number of redundancies in the sample set. Thus, this test was applied to examine a sample mean (i.e. TLS vectors) against a reference value (i.e. tacheometry vectors). Known as t-test, the analysis was performed using the formula [19]:

$$t = \frac{\bar{y} - \mu}{S/\sqrt{n}} \quad (5)$$

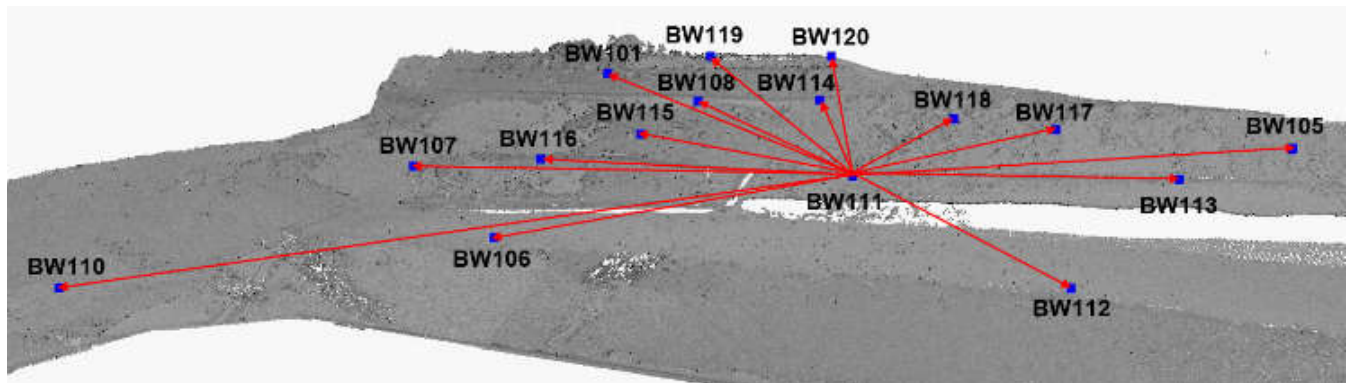


Fig. 8. Fifteen independent dimensions computed from sixteen targets.

where,

$\bar{y}$  = Sample mean

$\mu$  = Population mean

S = Standard deviation of the sample

n = Number of sample

The hypothesis of the test is:

$H_0$  : The sample mean is equal to the population mean

$H_A$  : The sample mean is not equal to the population mean

When the calculated t value as shown in (5) is larger than the value of critical t (predicted from the t-distribution table), the null hypothesis ( $H_0$ ) will be rejected with a selected level of significance (confidence level 95% equal to 0.05 of significance level). With the rejection of  $H_0$ , the sample mean is statistically different with population mean (accept  $H_A$ ).

#### D. Surface Deviation Analysis

Capability of TLSs to provide dense 3D data have allowed surface to surface comparison between two (2) set of data, which is known as surface deviation analysis. As visualised in Fig. 9, deviation of the surfaces were determined based on distances computed between each point of the compared cloud (epoch 02) and its nearest neighbour (point or triangle) in the reference entity (epoch 01).

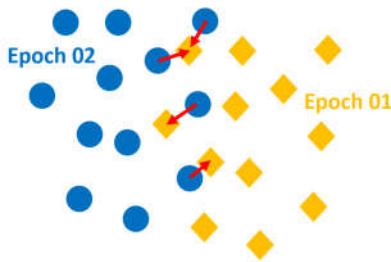


Fig. 9. Computation of distance for surface deviation analysis.

This study utilised CloudCompare open source software to perform surface deviation analysis for TLS first and second epoch data. Based on the computed distances of all surfaces, mean deviation can be yielded to represent average

displacement of the monitored surface. With the aim to investigate the significance of low vegetation effect in landslide surface deviation analysis, mean deviation obtained was statistically compared with mean displacement computed from DVs (yielded from artificial targets which were not affected by vegetation).

To ensure the study robustly examines the effect of low vegetation in TLS measurement, surface deviation experiment was designed based on the several interest regions. As illustrated in Fig. 10, there are three regions employed in this experiment: i) Region with less effect of high incidence angle (green area); ii) Region that contained all the sixteen artificial targets (blue area); and iii) Region with active land movement (grey area). Selection of regions were made by taking into account, the findings of previous two experiments (i.e. dimensional discrepancies and displacement vector assessment) which test the existence of uncertainties in TLS data due to the high incidence angle as well as distribution of ground control points (GCP). Based on that consideration, with the aid of Fig. 10, first region that only covers the area of nine artificial targets (green area) can be considered as the most accurate, followed by second level of accuracy region that covers all sixteen targets (blue area) and third region that covers all active motion area (grey area) has the worst accuracy amongst them.

Similar to the previous experiment, statistical analysis was employed to measure the effect of vegetation in TLSs land slope monitoring. The F-variance ratio test was used to investigate the significance of the similarity between two populations. The null hypothesis,  $H_0$ , of the test is that the two population variances are significantly similar while the alternate hypothesis is that they are different. The F-variance ratio test is defined as [19]:

$$F = \frac{\sigma_1^2}{\sigma_2^2} \quad (6)$$

Where,  $\sigma_1^2$  and  $\sigma_2^2$  are variances of the first and second populations, respectively. The null hypothesis is rejected if the calculated F value is larger than the critical F value (from

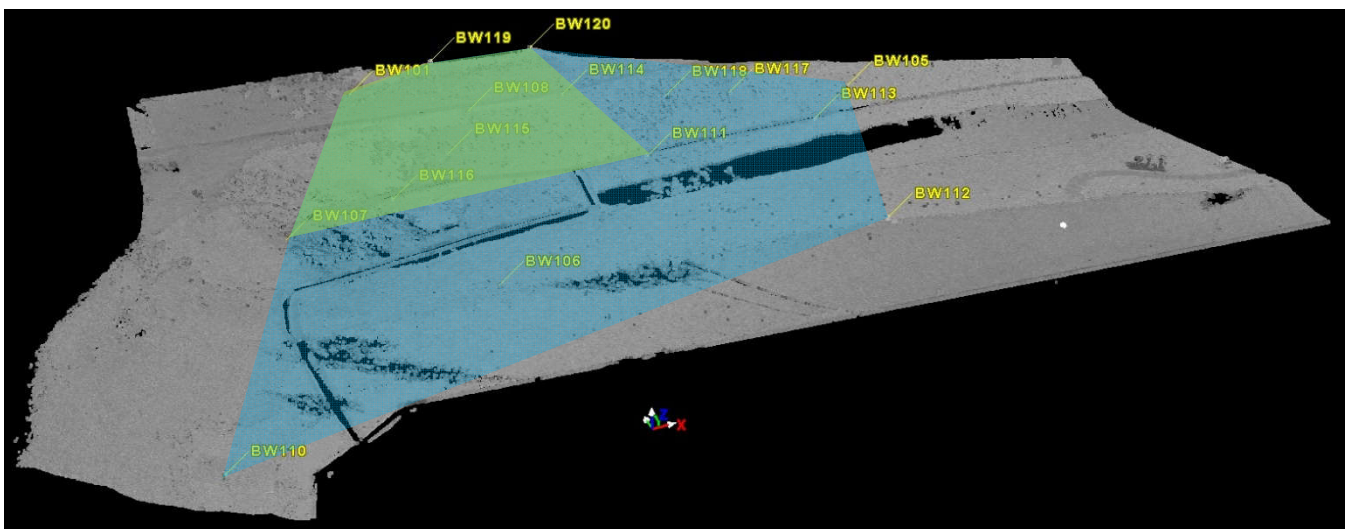


Fig. 10. Three regions exploited to measure the significant of low vegetation in TLS measurement.

the F-distribution table) at the 5% significance level. The rejection of  $H_0$  shows that the test parameters are not equal. If the null hypothesis is accepted in this test, then conclusion can be made that vegetation has no significant effect in TLS slope monitoring measurement.

IV. RESULTS AND ANALYSES

Assigned  $0.0014^\circ$  as precision for tacheometry angular measurement, least squares adjustment converged at third iteration. Reference standard deviation obtained from tacheometry observation is  $0.0027^\circ$ , which is equal to 2mm data quality for 50m range measurement. To evaluate the accuracy of Topcon GLS-2000 scanner data acquisition, there are three experiments that were performed: (1) Transformation similarity analysis; (2) Dimensional discrepancies; and (3) Displacement vector assessment. Results from these experiments can be employed to concretely verify the significance of vegetation effect in the final experiment (i.e. Surface deviation analysis).

In the first experiment, the finding utilised the adjusted values obtained from tacheometry (as reference value) to measure the accuracy of TLS data. Having sixteen well-distributed artificial targets, rigid body transformation algorithm was employed to performed coordinates transformation. Since the results from tacheometry are considered as a benchmark, targets from TLS data were transformed into photogrammetry points. After fourth iterations, the bundle adjustment converges and as presented in Table 1, the root mean square (RMS) of differences between control (tacheometry) and transformed coordinates for TLS data is 0.005m. With these outcomes, transformation similarity analysis has numerically demonstrated the significant quality of the examined TLS.

TABLE 1  
RMS OF DIFFERENCES BETWEEN CONTROL (TACHEOMETRY) AND TRANSFORMED COORDINATES (TLS DATA)

Axis	X (m)	Y (m)	Z (m)	XYZ (m)
Residual RMS	0.004	0.008	0.003	0.005

The second experiment exploited all the sixteen (16) targets by extracting fifteen independent vectors. To assess the accuracy of the TLS data, similar independent vectors were also yielded from the adjusted coordinates of tacheometry measurement. By differentiating the dimensions

produced from TLS data and tacheometry (reference value), the trend of accuracies obtained has been visually illustrated as depicted in Fig. 11. Through graphical assessment, TLS data has exhibited the consistent accuracy of 0.010m, except for vector BW111-BW110 that has yielded largest discrepancy (i.e. 0.020m). This situation is due to the fact that the occupied position for both instruments (i.e. TLS and tacheometry) are close to the target BW110 (as shown in Fig. 7), which caused high incidence angle in the measurement. For a concrete conclusion, statistical analysis was performed by calculating the standard deviation of TLS data. Based on the law of propagation of variance (LOPOV) algorithm, it was found that the accuracy of Topcon GLS-2000 scanner is 6mm. As expected, under 95% confidence interval (two sigma), the accuracy of the scanner as stated by the manufacturer is 7mm. This outcome had verified that the evaluated TLS manage to achieve accuracy which is sufficient to be implemented for land slope monitoring.

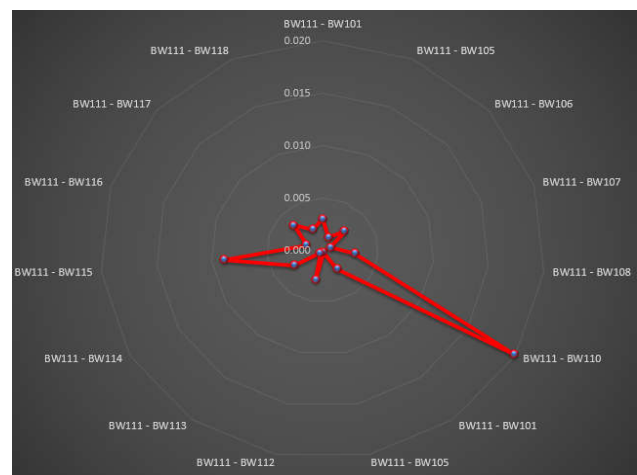


Fig. 11. The trend of errors obtained from TLS measurement.

Displacement vector analysis exploited two epochs measurement (with an interval of one month) for both instruments, TLS and tacheometry. Depicted in Fig. 12 is magnitudes and directions for all displacement vectors obtained from tacheometry and TLS measurements. Through graphic evaluation, all displacement vectors have shown a similar trend and consistent vectors for both measurement approaches except for targets BW112 and BW110, which have large direction contrast and vector discrepancy, respectively. In similar to previous experiment, it is expected

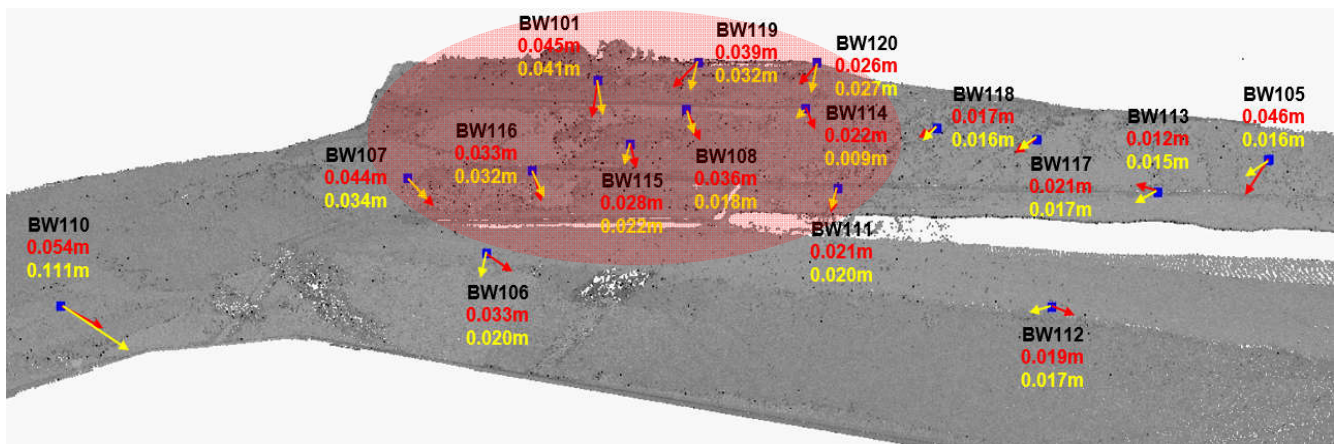


Fig. 12. Magnitude and direction of computed displacement vectors for both tacheometry and TLS data.

that the uncertainty that occurred may be due to the position of target which is quite close to the location of the sensors (refer Fig. 7). Thus, high incidence angle was expected to reduce the quality of measurement for targets that are near to the occupied sensors (e.g. BW112, BW106 and BW110). With the aid of LOPOV algorithm, computed mean displacement with the precision for tacheometry and TLS are  $0.028\text{m} \pm 0.006\text{m}$  and  $0.031\text{m} \pm 0.012\text{m}$ , respectively. Through similarity analysis using a t-test, the results indicate that calculated t is 1.015, while critical t obtained from the t-distribution table is 1.753. Since calculated t is smaller than critical t, thus, the null hypothesis is accepted. This finding has demonstrated strong agreement with the previous two experiments, where a conclusion can be made that TLS measurement is able to provide quality data similar to tacheometry measurement.

The final experiment was carried out to evaluate the capability of TLS in low vegetation slope monitoring. To ensure the integrity of computed point cloud displacement (known as surface deviation) from two epochs, mean displacement and precision of TLS measurement obtained from the third experiment were utilised as a benchmark. Furthermore, rigid evaluation was utilised in this final experiment by partitioning TLS data into three main regions which have three different accuracies. These variants occur due to the uncertainties in TLS measurement and distribution of network control employed in this study. The outcomes of surface deviation analyses for all the three regions have been organized and illustrated in Table 2 and Fig. 13, respectively.

TABLE 2  
SURFACE DEVIATION ANALYSES FOR THREE REGIONS

Region	Mean Distance (m)	Precision (m)
First (Fig. 13a)	0.041	$\pm 0.026\text{m}$
Second (Fig. 13b)	0.046	$\pm 0.030\text{m}$
Third (Fig. 13c)	0.060	$\pm 0.056\text{m}$

Exploiting F-variance ratio test, those standard deviations (or precision) were used to statistically examine the similarity of these three regions results with respect to TLS targets based outcome. As benchmark, the TLS targets-based approach that employed artificial targets have no effect of vegetation. Mathematically, it is obvious that the mean values have discrepancies of about 0.010m up to 0.029m as compared to tacheometry mean value (0.028m), TLS target-based approach gave 0.003m difference, while TLS surface based yielded 0.013m to 0.032m. Using Eq. (6), calculated F and critical F obtained for all three assessment have been presented in Table 3. Since calculated F are not in the 95% critical values accepted range, the null hypothesis is rejected.

TABLE 3  
SURFACE DEVIATION ANALYSES FOR THREE REGIONS

Region	Calculated F	Critical F	
		Lower	Upper
First (Fig. 14a)	0.223	0.418	1.833
Second (Fig. 14b)	0.167	0.418	1.833
Third (Fig. 14c)	0.048	0.418	1.833

With the various accuracies obtained in this final experiment, the findings have concretely indicated the significance of low vegetation effect on TLS surface deviation analysis. Furthermore, to ensure the quality of TLS measurement, it is advisable not to neglect the uncertainties contributed from vegetation. Disregarding the existence of vegetation in surface deviation analysis can cause fake deformation decision.

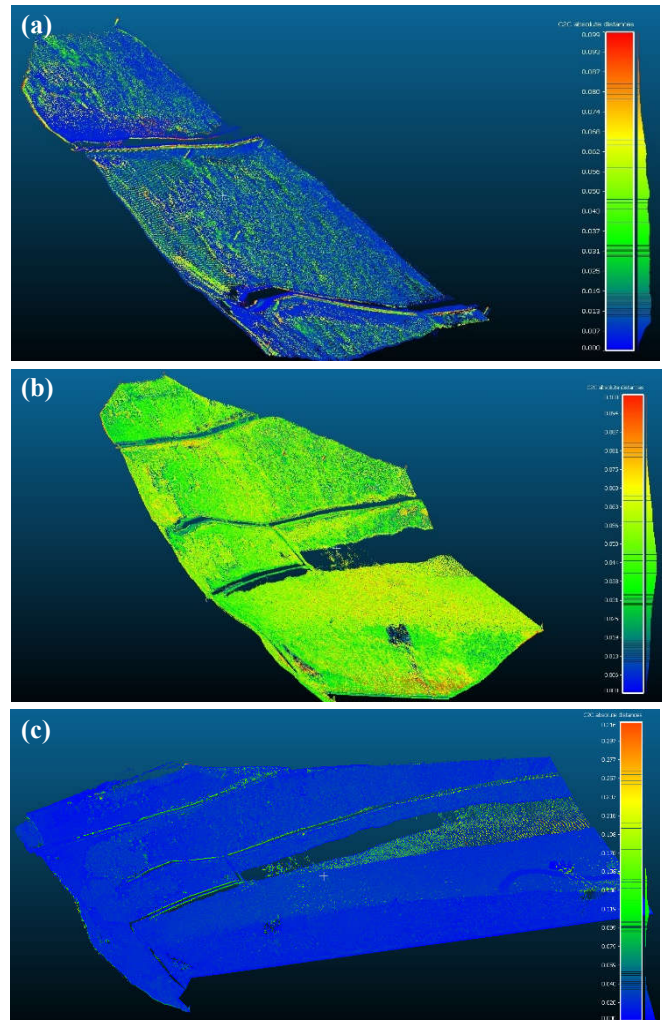


Fig. 13. Surface deviation analyses for first (a), second (b) and third (c) regions.

## V. CONCLUSION

The aim of this study is to examine the effect of vegetation uncertainties in the quality of TLS measurement. Rigid experiments were performed through surface deviation analysis to eventually conclude the significant of neglecting low vegetation effect on land slope. First, three experiments were designed to robustly evaluate the capability of TLS in landslide monitoring. Sixteen (16) artificial targets were well-distributed on the land slope and measured using tacheometry (for benchmarking) and TLS approaches. The first experiment yielded 5mm RMS from coordinate transformation procedure. This result indicates the significant similarity of the 3D coordinates for TLS and reference values (tacheometry). As claimed by manufacturer, with 95% confidence interval, the second experiment demonstrates that the accuracy of Topcon GLS-2000

scanner is 0.006m. The third experiment utilised data from two epochs of measurement to calculate displacement vectors. This is crucial in order to examine the reliability of TLS in deformation measurement (e.g. slope monitoring). With the aid of statistical analysis (i.e. t-test), similar to previous two experiments, TLS mathematically proved the capability to provide accurate data. However, the accuracy has been constrained by incidence angle when second and third experiments have indicated that two points showed large discrepancies in term of vector (BW110) and direction (BW112). It is essential to reduce the existence of high incidence angle by properly selecting the position of the scanner. Results obtained from the third experiment were used for final assessment to statistically evaluate the significance of vegetation in landslide monitoring. The F-variance ratio test has rejected the null hypothesis for all three regions which have different kind of accuracies (due to the uncertainties contributed from high incidence angle and distribution of GCP). To ascertain the use of surface deviation analysis for landslide monitoring, further study is crucial to model the vegetation uncertainties. Otherwise, this kind of analysis is only limited to the solid objects or structures (e.g. concrete dam, metal tank and engineering structure).

#### ACKNOWLEDGEMENT

We would like to thank the Universiti Teknologi MARA for the funding of this research. Our special thanks also go to Photogrammetry and Laser Scanning Research Group, Universiti Teknologi Malaysia for providing instruments and experimental site.

#### REFERENCES

- [1] L. M. Highland and P. Bobrowsky, (2008, November 15). *The landslide handbook - A guide to understanding landslides* (1st ver.) [online]. Available: <https://pubs.usgs.gov/circ/1325/>
- [2] R. N. Chowdhury and P. N. Flentje, "Geotechnical analysis of slopes and landslides - Achievements and challenges," in *11th IAEG Congress of the International Association of Engineering Geology and the Environment*, New Zealand, 2010, pp. 1-6.
- [3] A. G. Josep, C. Jordi and R. Joan, "Using global positioning system techniques in landslide monitoring," *Engineering Geology*, vol. 55, no. 3, pp. 167-192, Feb. 2000.
- [4] J. P. Malet, O. Maquaire and E. Calais, "The use of global positioning system techniques for the continuous monitoring of landslides: application to the super-sauze earthflow (alpes-de-haute-provence, France)," *Geomorphology*, vol. 43, no. 1, pp. 33-54, Feb. 2002.
- [5] I. T. Yang, J. K. Park and D. M. Kim, "Monitoring the symptoms of landslide using the non-prism total station," *KSCE Journal of Civil Engineering*, vol. 11, no. 6, pp. 293-301, Nov. 2007.
- [6] A. Wagner, "A new approach for geo-monitoring using modern total stations and RGB + D images," *Measurement*, vol. 82, pp. 64-74, Mar. 2016.
- [7] S. Mirzaee, M. Motagh and B. Akbari, "Landslide monitoring using InSAR time-series and GPS observations, case study: Shabkola landslide in northern Iran," *ISPRS - International Archives of the Photogrammetry, Remote Sensing and Spatial Information Sciences*, vol. XLII-1/W1, pp. 487-492, Jun. 2017.
- [8] A. Stumpf, J. P. Malet, P. Allemand, M. Pierrot-Deseilligny and G. Skupinski, "Ground-based multi-view photogrammetry for the monitoring of landslide deformation and erosion," *Geomorphology*, vol. 231, pp. 130-145, Feb. 2015.
- [9] M. V. Peppas, J. P. Mills, P. Moore, P. E. Miller and J. E. Chambers, "Accuracy assessment of a UAV-based landslide monitoring system," *ISPRS - International Archives of the Photogrammetry, Remote Sensing and Spatial Information Sciences*, vol. XLI-B5, pp. 895-902, Jul. 2016.
- [10] J. P. Malet, G. Ferhat, P. Ulrich, P. Boetzlé and J. Travelletti, "The French national landslide observatory OMIV-Monitoring surface displacement using permanent GNSS, photogrammetric cameras and terrestrial LiDAR for understanding the landslide mechanisms," in *Joint International Symposium on Deformation Monitoring (JISDM)*, Vienna, Austria, 2016, pp. 1-7.
- [11] Toyomi Fujita, and Toshinori Yoshida, "3D Terrain Sensing by Laser Range Finder with 4-DOF Sensor Movable Unit based on Frontier-Based Strategies," *Engineering Letters*, vol. 24, no.2, pp164-171, 2016
- [12] C. L. Lau, H. Setan, Z. Majid, M. A. Abbas, M. D. Ghazali and A. K. Chong, "An investigation of the optimal resolution for landslide monitoring using terrestrial laser scanner," in *FIG Congress 2014 Engaging the Challenges – Enhancing the Relevance*, Kuala Lumpur, Malaysia, pp. 1-13.
- [13] Y. Reshetyuk, "Self-calibration and direct georeferencing in terrestrial laser scanning," Ph.D. thesis, Department of Transport and Economics, Royal Institute of Technology (KTH), Stockholm, Sweden, 2009.
- [14] M. Barbarella, M. Fiani and A. Lugli, "Uncertainty in terrestrial laser scanner surveys of landslides," *Remote Sensing*, vol. 9, no. 2, pp. 113-140, Jan. 2017.
- [15] M. Alba, L. Barazzetti and M. Scaioni, "Filtering vegetation from terrestrial point clouds with low-cost near infrared cameras," *Italian Journal of Remote Sensing*, vol. 43, no. 2, pp. 55-75, Jun. 2011.
- [16] G. Sithole and G. Vosselman, "Comparison of filtering algorithms," in *Proceedings of the ISPRS Working Group III/3 Workshop 3-D Reconstruction from Airborne Laser Scanner and InSAR Data*, Dresden, Germany, 2003, pp. 71-78.
- [17] J. Szolomicki, "Application of 3D Laser Scanning to Computer Model of Historic Buildings," Lecture Notes in Engineering and Computer Science: Proceedings of The World Congress on Engineering and Computer Science 2015, WCECS 2015, 21-23 October, 2015, San Francisco, USA, pp858-863.
- [18] G. Tucci, G. Bartoli, M. Betti, V. Bonora, M. Korumaz and A. G. Korumaz, "Advanced procedure for documenting and assessment of cultural heritage: from laser scanning to finite element," in *IOP Conf. Series: Materials Science and Engineering*, vol. 364, pp. 1-10, Jun. 2018.
- [19] R. K. Napolitano, G. Scherer and B. Glisic, "Virtual tours and informational modeling for conservation of cultural heritage sites," *Journal of Cultural Heritage*, vol. 29, pp. 123-129, Jan. 2018.
- [20] Yuri A. Vershinin, "Digital Non-Contact Surface Reconstruction Scanner," Lecture Notes in Engineering and Computer Science: Proceeding of the International MultiConference of Engineers and Computer Scientists 2013, IMECS 2013, 13-15 March, 2013, Hong Kong, pp478-483.
- [21] Nallig Leal, Esmeide Leal, and Sanchez-Torres German, "A Linear Programming Approach for 3D Point Cloud Simplification," *IAENG International Journal of Computer Science*, vol. 44, no.1, pp60-67, 2017
- [22] AHM Zahirul Alam, Noor Syamira Asyiqin Amir Hassan, Nurul Arfah Che Mustapha, Md Rafiqul Islam, Sheroz Khan, and Muhammad Abu Eusuf, "Wireless Capacitor Sensing for Structural Health Monitor," Lecture Notes in Engineering and Computer Science: Proceedings of The World Congress on Engineering 2016, WCE 2016, 29 June - 1 July, 2016, London, U.K., pp319-321.
- [23] X. Xu, H. Yang and I. Neumann, "Deformation monitoring of typical composite structures based on terrestrial laser scanning technology," *Composite Structures*, vol. 202, pp. 77-81, Oct. 2018.
- [24] H. Yang, X. Xu, and I. Neumann, "Optimal finite element model with response surface methodology for concrete based on terrestrial laser scanning technology," *Composite Structures*, vol. 183, pp. 2-6, Jan. 2018.
- [25] H. González-Jorge, B. Riveiro, P. Arias and J. Armesto, "Photogrammetry and laser scanner technology applied to length measurements in car testing laboratories," *Measurement*, vol. 45, no. 3, pp. 354-363, Apr. 2012.
- [26] M. Popia (Ilica). (2013). Terrestrial laser scanning technology used in the field of shipbuilding. *RevCAD Journal of Geodesy and Cadastre* [online]. 15(14). pp. 121-128. Available: [http://www.revcad.uab.ro/index.php?pagina=pg&id=3&rev=da&id\\_rev=34&modul=rev](http://www.revcad.uab.ro/index.php?pagina=pg&id=3&rev=da&id_rev=34&modul=rev)
- [27] M. A. Abbas, L. C. Luh, H. Setan, Z. Majid, A. K. Chong, A. Aspuri, K. M. Idris and M. F. M. Ariff, "Terrestrial laser scanners pre-



processing: registration and georeferencing.” *Jurnal Teknologi*, vol. 71, no. 4, pp. 115–122, Dec. 2014.

- [28] Jae Hoon Lee, Shingo Okamoto, Yuki Yoshi Uchida, and Yasuaki Yamaguchi, “Development of a Height Measurement System based on 2D Laser Scan,” *Lecture Notes in Engineering and Computer Science: Proceeding of the International MultiConference of Engineers and Computer Scientists 2012, IMECS 2012*, 14-16 March, 2012, Hong Kong, pp340-343.
- [29] C. D. Ghilani. (2010, March 9). *Adjustment computations: spatial data analysis* (5th ed.) [online]. Available: <https://www.onlinelibrary.wiley.com/doi/book/10.1002/9780470586266>